Hindawi
Adsorption Science & Technology
Volume 2022, Article ID 1853758, 10 pages
https://doi.org/10.1155/2022/1853758

Research Article

Methylene Blue Removal by Chitosan Cross-Linked Zeolite from Aqueous Solution and Other Ion Effects: Isotherm, Kinetic, and Desorption Studies

Endar Hidayat, Seiichiro Yonemura, Yoshiharu Mitoma, and Hiroyuki Harada

Graduate School of Comprehensive and Scientific Research, Prefectural University of Hiroshima, Japan

Correspondence should be addressed to Hiroyuki Harada; ho-harada@pu-hiroshima.ac.jp

Received 19 August 2022; Accepted 10 October 2022; Published 27 October 2022

Academic Editor: Chinenye Adaobi Igwegbe

Developing innovative technology for removing methylene blue (MB) from water is essential since the widespread discharge of MB from industrial effluents causes problems for humans and the environment. In this study, we conducted the adsorption method, a simple technique that utilizes an adsorbent. Chitosan is cross-linked with zeolite as a promising adsorbent material and environmentally friendly. For the characterization, FTIR, SEM-EDS, DLS, and pH_{zpc} were analyzed. It was discovered that the removal percentage reached 97% with an adsorption capacity of 242.51 mg/g for 60 minutes at pH 10. The adsorption isotherm and kinetic model were investigated. As a result, the Freundlich model and pseudo-second-order model were fitted to the adsorption process. Moreover, the effect of other ions was investigated for 5 minutes of mixing time. The results showed that the removal percentage increased in the presence of H_2O_2 ion. Contrary to sodium chloride, glucose, and citric acid ions, the effectiveness of H_2SO_4 as a desorbing agent was 99.65% for 30 minutes at 45°C.

1. Introduction

The use of dyes in industry generates a considerable amount of printing and dyeing wastewater, which is harmful to the environment and human health [1, 2]. Methylene blue (MB) is a cationic dye that is often used as a coloring agent, medicine, and chemical indicator [3]. MB was detected in either low or high amounts in the effluents [4]. However, dye is a hazardous chemical whose breakdown may cause water contamination. Therefore, scientists have developed various physical, chemical, and biological ways to remove the dye from the water. Adsorption is a common technique for dye removal from an aqueous solution due to its simplicity and low cost.

Zeolites attract significant attention due to their high surface area and porous structure with exchangeable cations [5, 6]. Zeolite is a crystalline aluminosilicate with a 3D structure linked to oxygen atoms [7]. Additionally, zeolites may be recycled and reused several times [8]. However, zeolites cannot be used for dye adsorption since their adsorption ability decreases with time. As a result, modifying zeolite is a method for increasing dye removal. To overcome these constraints, chitosan was utilized as a cross-linking agent. Chitosan is a unique polymer that is nontoxic to the environment, has an abundance of functional groups (amino, methyl, and hydroxyl groups), and is simple to modify or react with other compounds [9].

Several researchers have reportedly used chitosan modified for dye removal [10–12]. However, there are no reports of using chitosan cross-linked with zeolite as an adsorbent to remove MB from water. The current study investigated the influence of pH, initial MB concentration, adsorbent dosage, contact time, and other ions such as NaCl, glucose, citric acid, and H_2O_2 on MB adsorption.

2. Materials and Methods

2.1. Materials. Zeolite synthetic (ZL) was from previous research [6]. Methylene blue (MB), chitosan (CH), sodium hydroxide (NaOH), hydrochloric acid (HCl), sulfuric acid (H_2SO_4), citric acid ($C_6H_8O_7$), D^+ glucose ($C_6H_{12}O_6$), sodium chloride (NaCl), and hydrogen peroxide (H_2O_2) were purchased from Kanto Chemical Co. Inc. (Tokyo, Japan). EDTA-Na solution was purchased from Dojindo Moleculer Technologies, Inc. (Tokyo, Japan). The MB characteristics are shown in Table 1.

2.2. Preparation of Adsorbent. The adsorbent preparation followed previous research with modifications [6]. The process was conducted at room temperature. Chitosan was mixed with different ratios of acetic acid 0.5 : 1 and 1 : 1, referred to as ZLCH-a and ZLCH-b, respectively. 1 g of zeolite was mixed with 25 mL of chitosan solution for two hours (Rotator RT-50). Afterward, 25 mL of 1 M NaOH was added and mixed for thirty minutes. Then filtered, and dried at 60°C for 48 hours. Lastly, the adsorbent was sieved at <100 μm.

2.3. Adsorption Experiments. All experiments were conducted for three replicates on a magnetic stirrer at room temperature (25°C). The pH effect, adsorbent dose, initial MB concentration, and contact time on the adsorption of MB were investigated. The adsorption capacity and percent removal were calculated using the following equations, respectively.

$$q_e = \frac{C_o - C_e}{W} V, \tag{1}$$

$$\%\text{Removal} = \frac{C_o - C_e}{C_0} 100, \tag{2}$$

where q_e is the adsorption capacity (mg/g), C_o is the initial MB concentration (mg/L), C_e is the equilibrium of MB (mg/L), W is the adsorbent mass (g), and V is the volume of MB (L).

2.4. Adsorption Kinetics. ZLCH-b was mixed with 100 mL (25 mg/L of MB) in intervals time from 1 to 60 minutes. The adsorption capacity at the time was calculated using the following equation.

$$q_e = \frac{C_o - C_t}{W} V, \tag{3}$$

where C_t is the MB concentration at time (min) (mg/L), C_o is the initial concentration of MB (mg/L), W is adsorbent mass (g), and V is the volume of MB solution (L).

2.5. The pH of Zero Point Charge. The salt addition was employed to determine the pH of the zero point charge of the ZLCH-b. A constant amount of solute was added to a series of solutions containing different pH strengths [13]. In a 100 mL beaker, 0.1 g of ZLCH-b was distributed in a 50 mL solution containing 0.01 M NaCl. 0.01 M HCL and 0.01 M NaOH were used for pH adjustment in acidic and alkaline conditions. The samples were agitated for 24 hours using a rotary agitator (Rotator RT-50). The point zero charges were calculated by plotting ΔpH (pH final − pH initial) versus pH initial.

2.6. Desorption Studies. Under optimal conditions of MB adsorption, desorption studies were employed. 25 mg/L of MB-loaded to ZLCH-b at pH 10. It was soaked in 0.01 M (NaOH, EDTA-Na, HCl, and H_2SO_4). The desorption percentage is calculated using the following equation.

$$\%\text{desorption} = \frac{C_{ed}}{C_i - C_e} \times 100, \tag{4}$$

where %desorption is the desorption percentage (%), C_i is the initial MB concentration before adsorption (mg/L), C_e is the equilibrium MB concentration after adsorption (mg/L), and C_{ed} is the equilibrium MB concentration after desorption (mg/L).

2.7. Characterization. MB concentration was analyzed using a UV-Vis spectrophotometer (Jasco V-530, Jasco Corporation, Tokyo, Japan). The functional group of the adsorbent was investigated by ATR-FTIR in the region of 400–4000 cm^{-1} before and after adsorption at 1 cm^{-1} (Thermo Scientific Nicolet iS10, Thermo Fisher Scientific Inc., Waltham, MA, USA). The photograph and EDS data were analyzed using scanning electron microscopy (SEM) (Hitachi TM3000, Tokyo, Japan) and SEM-EDS (JIED-2300, Shimadzu, Kyoto, Japan), respectively. The original unit results of specific surface area (SSA) are cm^2/cm^3 and converted to m^2/g with assumed cm^3 = g. It was analyzed using dynamic light scattering (DLS) (Horiba LB-550, Kyoto, Japan).

3. Results and Discussion

3.1. Adsorbent Characteristics. The SEM images and EDS spectra of the adsorbent (ZLCH-a and ZLCH-b) are shown in Figure 1. As can be seen, both surface adsorbents had interlayers, containing porous and adhesive structures. The EDS data revealed that the value of carbon and sodium in ZLCH-a is higher than that in ZLCH-b. By comparing SSA data (Table 2), it can be concluded that ZLCH-b shows the lowest result than ZLCH-a from 96.85 mg/g to 88.51 mg/g, respectively (data not shown), indicating that ZLCH-b had much of the mass unit number. The mass unit number has correlated with the adsorbent sites to catch the number of the ions. It could confirm the adsorption process's effectiveness (Figure 2). Hence, ZLCH-b was used for the next treatment.

3.2. Optimum pH. The pH of the dye solution is critical to the adsorption capacity mechanisms [14]. The influence of pH on the MB adsorption onto ZLCH-b with an initial MB concentration of 10 mg/L is shown in Figure 2(a). The result shows that the adsorption capacity and removal percentage increased from 37.68 to 97.35 mg/g and 37.7 to 97.3%, respectively, when the initial pH was changed from 2 to 10. It could be confirmed with the pH zero point charge of the adsorbent (Figure 2(b)). When the pH is below pH_{zpc},

Table 1: General characteristics of MB.

Characteristics	AR88	Chemical structure
General name	Methylene blue	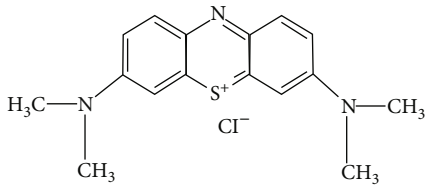
Molecular weight	319.85	
Chemical formula	$C_{16}H_{18}ClN_3S$	
Dye type	Thiazine	
Nature	Cationic	
λ max (nm)	665	

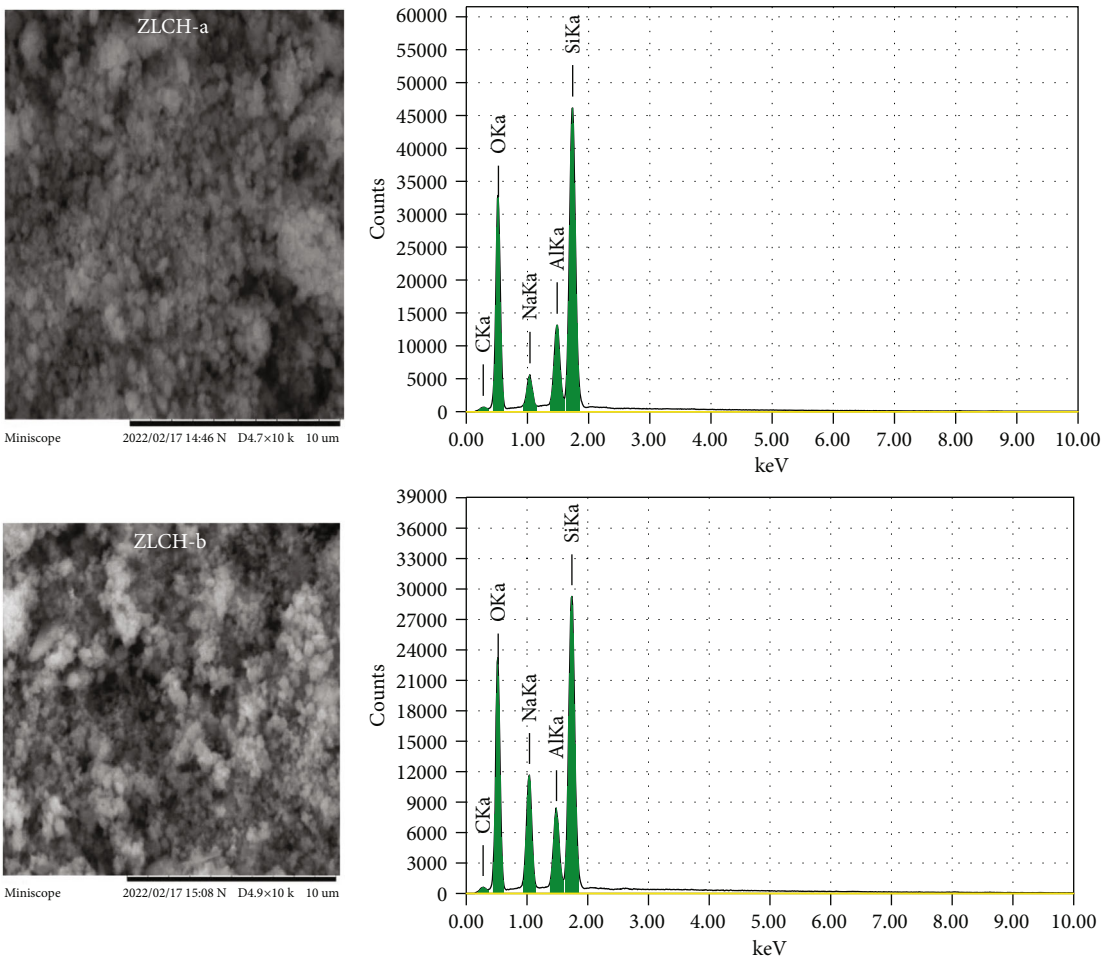

Figure 1: SEM images and EDS spectra of ZLCH-a and ZLCH-b.

Table 2: Element data and specific surface area of ZLCH-a and ZLCH-b.

Parameters (wt%)	ZLCH-a	ZLCH-b
Carbon (C)	2.60	3.11
Oxygen (O)	49.15	45.37
Sodium (Na)	4.11	12.69
Aluminium (Al)	9.08	7.99
Silica (Si)	35.07	30.84
Specific surface area (SSA) (m^2/g)	5.98	1.08

the surface charge of the adsorbent may become positively charged, forcing H^+ ions to compete with MB cations, resulting in a decrease in the amount of dye adsorbed (Azza [15, 16]). However, when the pH is above pH_{zpc}, the surface charge becomes negatively charged favouring MB removal. This result is similar to Maryam et al. [14] for MB removal by corn husk carbon activation $ZnCl_2$.

3.3. Effects of Initial MB Concentration. The effect of initial MB concentration (10-25 mg/L) on the MB adsorption onto ZLCH-b is shown in Figure 3. The adsorption capacity increased with increasing initial MB concentration from 97.35 to 207.16 mg/g, and the removal percentage decreased

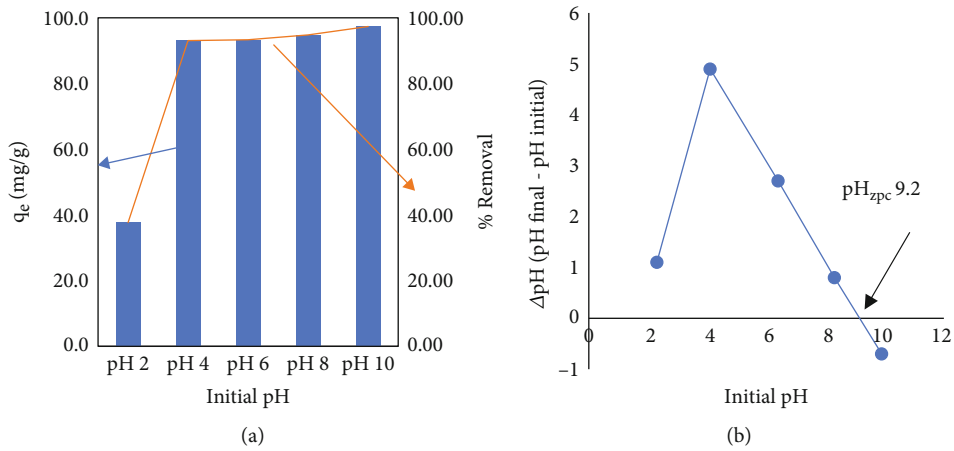

Figure 2: (a) Initial pH effects on MB adsorption capacity and removal percentage. (b) pH zero point charge of ZLCH-b.

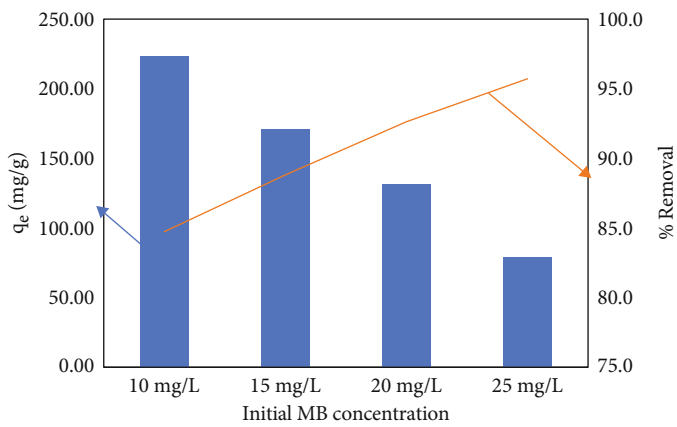

Figure 3: Initial MB concentrations affect adsorption capacity and removal percentage.

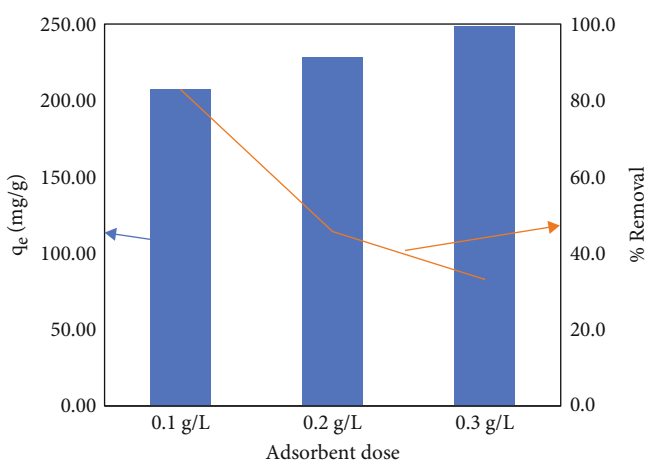

Figure 4: Adsorbent doses affect MB adsorption capacity and removal percentage.

with the increase in initial MB concentration from 97.3 to 82.9%. It may cause the ratio of the initial number of MB molecules to the surface area to be low at lower concentrations [14]. However, at high concentrations, the number of accessible adsorption sites decreases. Hence, the removal percentage depends on the initial concentration [6].

3.4. Effects of Adsorbent Doses. Getting a higher amount of adsorption capacity with the lowest adsorbent dose is essential for eliminating contaminants [17]. Figure 4 shows the effect of adsorbent dose from 0.1 to 0.3 g/L on ZLCH-b adsorption. As a result, the impact on adsorption capacity decreased with the increasing dose from 207.16 to 82.86 mg/

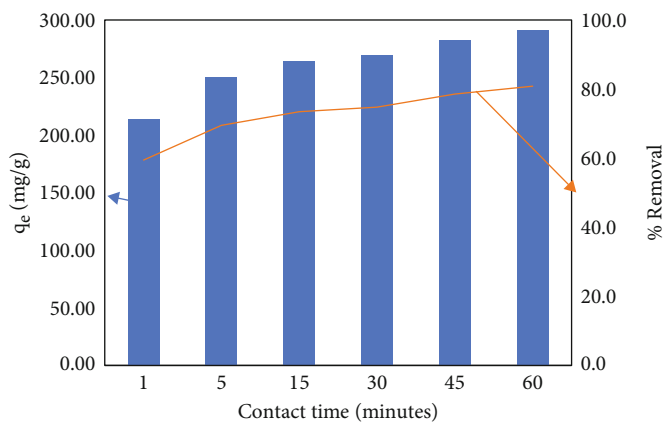

Figure 5: Contact time affects MB adsorption capacity and removal percentage.

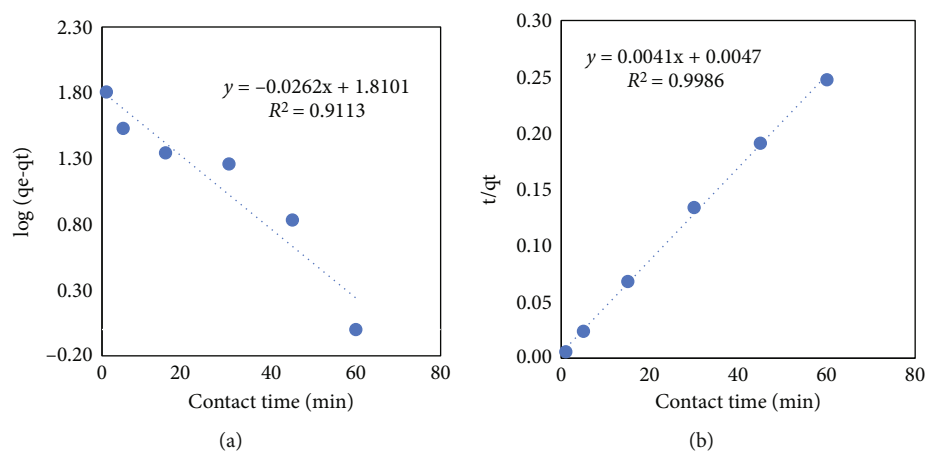

Figure 6: Adsorption kinetic model of MB by ZLCH-b. (a) Pseudo-first order. (b) Pseudo-second order.

Table 3: Pseudo-first- and pseudo-second-order kinetic model of MB adsorption onto ZLCH-b adsorbent.

Pseudo-first order			Pseudo-second order		
q_e	K_1	R^2	q_e	K_2	R^2
6.11	-0.0004	0.9113	243.90	0.003	0.9978

g, and the removal percentage increased from 82.9 to 99.4%. Similar results have been reported for dye removal [18, 19]. The decrement of MB adsorption capacity at a higher dose of adsorbent is because active adsorbent sites are less accessible due to adsorbent particles collected and overlapped [20], while the increment of the removal percentage due to the increased number of binding sites would lead to a decrease in the total surface area of the adsorbent [21, 22].

3.5. Effects of Contact Time. As shown in Figure 5, the effect of contact time on the adsorption capacity of ZLCH-b for MB removal was studied between 1 and 60 minutes. The result indicates that the removal percentage increases rapidly from 0 to 1 minute (71.3%) and then gradually up to 60 minutes (97%), indicating that the electrostatic interaction between MB and adsorbent is responsible, and MB molecules were caught and filled up in the adsorbent sites.

3.6. Adsorption Kinetic Studies. Adsorption kinetic studies are important to provide information on the MB adsorption mechanism onto ZLCH-b. The most commonly used are pseudo-first- and pseudo-second-order kinetic models [6, 23, 24]. The experimental data of kinetic studies for first and second order are illustrated in Figures 6(a) and 6(b), respectively. Pseudo-first-order and pseudo-second-order kinetic models are shown in the following equations (5) and (6), respectively

$$\log(q_e - q_t) = \log q_e - K_1 t, \tag{5}$$

$$\frac{t}{q_t} = \frac{1}{K_2 q^2 q_e} + \frac{t}{q_e}. \tag{6}$$

Table 3 shows the correlation linear of the pseudo-first- and pseudo-second-order kinetic models ($R^2 = 0.9113$ and $R^2 = 0.9978$), respectively, indicating that the pseudo-second-order kinetic model fits onto the ZLCH-b adsorption process.

3.7. Adsorption Isotherm Studies. In the current study, we used the Langmuir and Freundlich adsorption isotherm models, which are common by many authors [6, 25, 26]. Langmuir occurs on the single layer of the adsorbent surface,

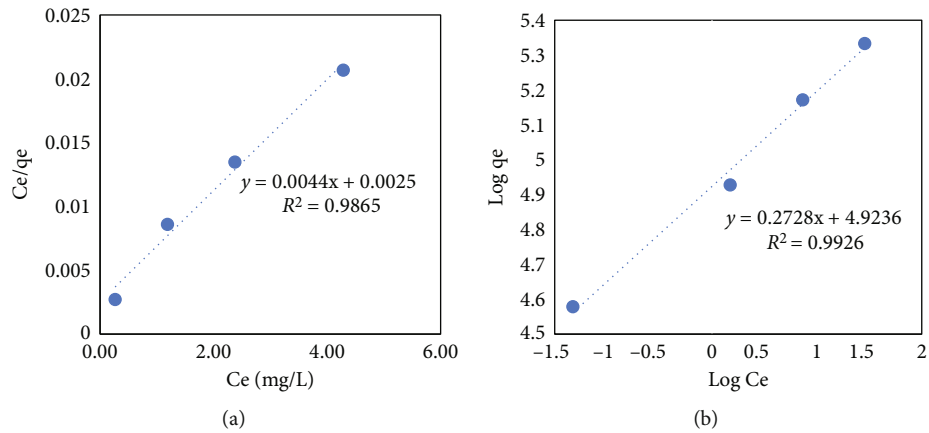

Figure 7: Adsorption isotherm model of MB by ZLCH-b. (a) Langmuir isotherm. (b) Freundlich isotherm.

Table 4: Langmuir and Freundlich's isotherm models of MB adsorption onto ZLCH-b.

	Langmuir parameters			Freundlich parameters		
q_{max}	K_1	R^2	R_L	K_f	n	R^2
229.60	394.24	0.9865	0.00002	83860	0.27	0.9926

while Freundlich on the multilayer of the adsorbent surface. The equation for Langmuir (7), Langmuir separation factor characteristics (8), and Freundlich (9) are shown in below:

$$\frac{C_e}{q_e} = \frac{(C_e/q_{max}) + 1}{K_1 q_{max}}, \tag{7}$$

$$R_L = \left(\frac{1}{1 + bC_o}\right), \tag{8}$$

$$\ln_{q_e} = \ln K_f + \frac{1}{n} \times \ln C_e, \tag{9}$$

where q_e is the adsorbent amount (mg/g), q_t is the equilibrium time (mg/g), K_1 is the adsorption equilibrium constant (L/mg), q_{max} is the single layer of maximal adsorption capacity, and C_e is the equilibrium concentration (mg/L). R_L is the equilibrium parameter of Langmuir characteristics. K_f is the multilayer of absorption capacity (mg/g), and n is the adsorption intensity.

The experimental adsorption isotherm data for Langmuir, Freundlich, and the correlation coefficient of MB are shown in Figures 7(a) and 7(b) and Table 4, respectively. As a result, the R^2 value of Freundlich was higher than the Langmuir isotherm model and the value of R_L in these studies (0.00002), indicating that the adsorption isotherm of MB onto ZLCH-b is a Freundlich isotherm model and favorable [27].

3.8. Influence of Ion Strength. The influence of other ions on the MB adsorption is essential because the water solution in the environment has diverse ions as shown in Figure 8. 0.1 g/L of adsorbent, 25 mg/L MB, and 50 mg/L (sodium chloride, glucose, citric acid, and H_2O_2) were investigated. The adsorption process was conducted on a magnetic stirrer for 5 minutes. We found that the removal percentage decreased by adding citric acid, sodium chloride, and glucose. This is due to the surface of the adsorbent competing with other ions which inhibited MB molecules trapped on the adsorbent surface sites. In contrast, the removal percentage increased by adding H_2O_2 compared with no contaminant from 83.4 to 85.3%, respectively, which indicates that an oxidation reaction simultaneously occurred with the adsorption process. The proposed mechanism's interaction is shown in Figure 9.

3.9. FTIR Data. The FTIR spectra of the adsorbent before and after MB adsorption in the absence of other ions are shown in Figure 10. After the MB adsorption process, the range and intensity of peaks in the adsorbent structure were changed, which could be due to the interaction and placement of the MB on the adsorbent surface. For example, after the adsorption process, the range of –OH vibrations in the ZLCH-b increased to 3363 cm^{-1}, indicating that hydrogen bonds have been formed in the adsorption process. A decreased band peak was found from 1645 to 1604 cm^{-1}, which corresponded to the N-H group, resulting in increased electrostatic interaction between MB and the ZLCH-b adsorbent [6]. Moreover, the other peaks in the band also decreased after the adsorption process, from 1423 to 1393 cm^{-1}. It may cause N-O stretching to correspond to C-H in OH- or NH_2 groups. The band from 1050 to 950 cm^{-1} was assigned to the internal asymmetric stretching of Si-O-Si or Si-O-Al [28]. New peaks after adsorption were found at 2924 and 1731 cm^{-1}, which corresponded to C-H and C=O, respectively [29].

3.10. Desorption Studies. MB recovery is important in economic terms. Desorption of percentage with various solvents is shown in Figure 11(a). As can be seen, using an alkaline agent (NaOH), the desorption percentage reached 1.64%. While using an acidic agent (HCl and H_2SO_4), the desorption percentage reached 49.75% and 57.05%, respectively. This is due to hydrochloric acid having one proton, whereas sulfuric acid contains two protons, making sulfuric acid more effective in separating (-OH) from the NH_2- to H^+ of ZLCH-b. After that, sulfuric acid is employed as the subsequent treatment

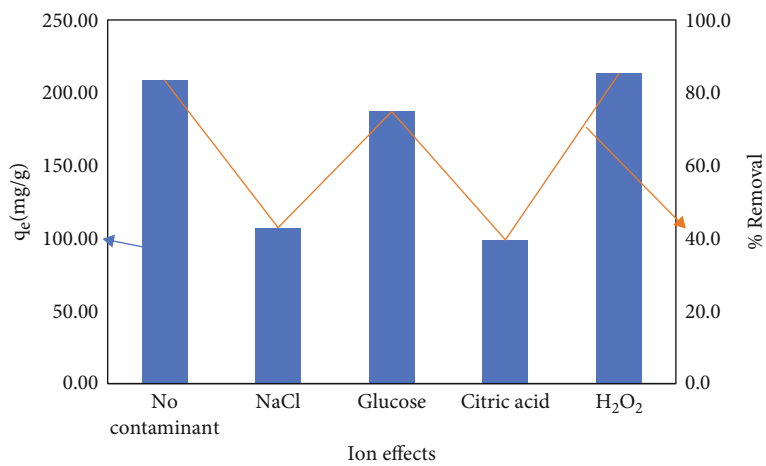

Figure 8: Ion effects on MB adsorption capacity and removal percentage.

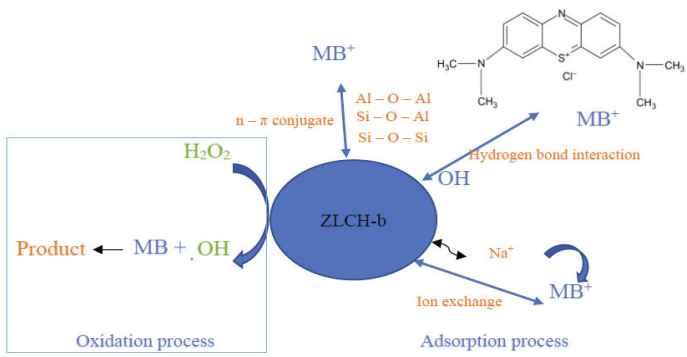

Figure 9: The proposed mechanisms of adsorption and oxidation simultaneously.

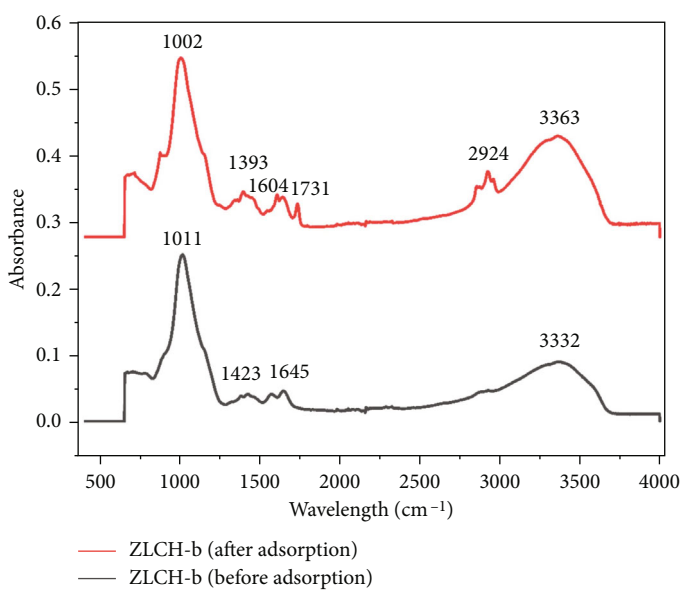

Figure 10: The ATR-FTIR analysis of ZLCH-b before and after MB adsorption.

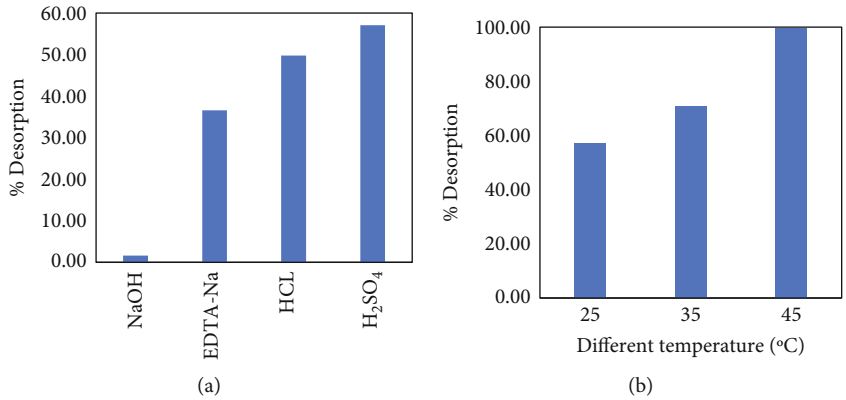

Figure 11: Desorption percentage: (a) different desorbing agents and (b) different temperatures using H_2SO_4.

Table 5: Several adsorbent performances on MB removal.

Adsorbent	Initial MB concentration (mg/L)	Adsorption capacity (mg/g)	References
Fava bean peels	25	140	Bayomie et al. [31]
Zeolite-activated carbon from oil palm ash	400	285.71	Khanday et al. [8]
Mesoporous-activated carbon (CSAC) from chitosan flakes	400	143.53	Marrakchi et al. [32]
Coconut shell	200	50.6	Jawad et al. [33]
Wild carrot	25	21	Swamy et al. [34]
Acid-treated banana peel (ATBP)	300	250	Jawad et al. [35]
ZLCH-b	25	252.51	This study

(Figure 11(b)). Due to the low percentage results, we increased the temperature. The results obtained that the desorption percentage increased to 99.65% at 45°C. This indicates that oxidizing plays an important role in releasing hydrogen groups from adsorbent surface. This agrees with Momina et al. [30] for the desorption of MB from bentonite adsorbent coating.

3.11. Comparison with Other Results. Table 5 shows the comparison of the adsorption capacity of MB using several adsorbents. We can see that the highest adsorption capacity derived from zeolite-activated carbon from oil palm ash was 285.71 mg/g with an initial MB concentration of 400 mg/L. However, our study reaches 252.51 mg/g with an initial MB concentration of 25 mg/L. These results concluded that ZLCH could be practical to remove MB from water.

4. Conclusion

Zeolite modified was evaluated and confirmed to be a promising adsorbent for MB removal from water. MB removal has been studied under various experimental conditions. The result shows that increased pH and initial MB concentration would increase the adsorption capacity, while increased adsorbent dose would decrease the adsorption capacity. Experimental data showed the Freundlich isotherm and pseudo-second-order kinetic models. The effect of sodium chloride, glucose, and citric acid could decrease the removal percentage. However, it increased after adding the H_2O_2 ion. These results indicate that adsorption and oxidation processes simultaneously occurred for MB removal. MB desorption was efficient used sulfuric acid.

Data Availability

The previous adsorbent data (ZLCH-b) used to support the findings of this study have been deposited in the [6] repository 10.3390/polym14050893.

Conflicts of Interest

The authors declare that they have no conflicts of interest.

Acknowledgments

The authors (E.H.) express gratitude to the MEXT scholarship for sponsoring the studies at the Prefectural University of Hiroshima, Japan.

References

[1] H. Ma, P. Shengyan, H. Yaqi, R. Zhu, Z. Anatoly, and C. Wei, "A highly efficient magnetic chitosan "fluid" adsorbent with a high capacity and fast adsorption kinetics for dyeing wastewater purification," *Chemical Engineering Journal*, vol. 345, pp. 556–565, 2018.

[2] Y. Zhu, B. Yi, Q. Yuan, Y. Wu, M. Wang, and S. Yan, "Removal of methylene blue from aqueous solution by cattle manure-

derived low temperature biochar," *RSC Advances*, vol. 8, no. 36, pp. 19917–19929, 2018.

[3] L. Liu, Y. Li, and S. Fan, "Preparation of KOH and H_3PO_4 modified biochar and its application in methylene blue removal from aqueous solution," *Processes*, vol. 7, no. 12, p. 891, 2019.

[4] L. Gong, W. Sun, and L. Kong, "Adsorption of methylene blue by NaOH-modified dead leaves of plane trees," *Computational Water, Energy, and Environmental Engineering*, vol. 2, no. 2, pp. 13–19, 2013, 10.4236/cweee.2013.22B003.

[5] A. Iryani, A. Masudi, A. I. Rozafia et al., "Enhanced removal of soluble and insoluble dyes over hierarchical zeolites: effect of synthesis condition," *Inorganics*, vol. 8, no. 9, p. 52, 2020.

[6] E. Hidayat, H. Harada, Y. Mitoma, S. Yonemura, and H. I. A Halem, "Rapid removal of acid red 88 by zeolite/chitosan hydrogel in aqueous solution," *Polymers*, vol. 14, no. 5, p. 893, 2022.

[7] C. Belviso, "Zeolite for potential toxic metal uptake from contaminated soil: a brief review," *Processes*, vol. 8, no. 7, p. 820, 2020.

[8] W. A. Khanday, F. Marrakchi, M. Asif, and B. H. Hameed, "Mesoporous zeolite–activated carbon composite from oil palm ash as an effective adsorbent for methylene blue," *Journal of the Taiwan Institute of Chemical Engineers*, vol. 70, pp. 32–41, 2017.

[9] L. Shao and C. Qi, "Chitosan microspheres-supported palladium species as an efficient and recyclable catalyst for Mizoroki-Heck reaction," *New Journal of Chemistry*, vol. 41, no. 16, pp. 8156–8165, 2017.

[10] A. H. Jawad, A. S. Abdulhameed, R. Selvasembian, Z. A. ALOthman, and L. D. Wilson, "Magnetic biohybrid chitosan-ethylene glycol diglycidyl ether/magnesium oxide/Fe_3O_4 nanocomposite for textile dye removal: Box-Behnken design optimization and mechanism study," *Journal of Polymer Research*, vol. 29, no. 5, 2022.

[11] I. Rahmi and I. Mustafa, "Methylene blue removal from water using H_2SO_4 crosslinked magnetic chitosan nanocomposite beads," *Microchemical Journal*, vol. 144, no. 1, pp. 397–402, 2019.

[12] S. Zhao, F. Zhou, L. Li, M. Cao, D. Zuo, and H. Liu, "Removal of anionic dyes from aqueous solution by adsorption of chitosan-based semi-IPN hydrogel composites," *Composites Part B: Engineering*, vol. 43, no. 3, pp. 1570–1578, 2012.

[13] T. Mahmood, M. T. Saddique, A. Naeem, P. Westerhoff, S. Mustafa, and A. Alum, "Comparison of different methods for the point of zero charge determination of NiO," vol. 50, no. 17, pp. 10017–10023, 2011.

[14] M. Khodaie, N. Ghasemi, B. Moradi, and M. Rahimi, "Removal of methylene blue from wastewater by adsorption on ZnCl2 activated corn husk carbon equilibrium studies," *Journal of Chemistry*, vol. 2013, Article ID 383985, 6 pages, 2013.

[15] A. El-Maghraby and H. A. El Deeb, "Removal of a basic dye from aqueous solution by adsorption using rice hulls," *Global Nest Journal*, vol. 13, no. 1, pp. 90–98, 2011.

[16] C. H. Lai and C. Y. Chen, "Removal of metal ions and humic acid from water by iron-coated filter media," *Chemosphere*, vol. 44, no. 5, pp. 1177–1184, 2001.

[17] H. Mittal, V. Kumar, Saruchi, and S. S. Ray, "Adsorption of methyl violet from aqueous solution using gum xanthan/Fe_3O_4 based nanocomposite hydrogel," *International Journal of Biological Macromolecules*, vol. 89, pp. 1–11, 2016.

[18] A. A. El-Bindary, A. Z. El-Sonbati, A. A. Al-Sarawy, K. S. Mohamed, and M. A. Farid, "Adsorption and thermodynamic studies of hazardous azocoumarin dye from an aqueous solution onto low cost rice straw based carbons," *Journal of Molecular Liquids*, vol. 199, pp. 71–78, 2014.

[19] V. S. Mane and P. V. Vijay Babu, "Kinetic and equilibrium studies on the removal of Congo red from aqueous solution using eucalyptus wood (Eucalyptus globulus) saw dust," *Journal of Taiwan Institute of Chemical Engineers*, vol. 44, no. 1, pp. 81–88, 2013, 10.1016/j.jtice.2012.09.013.

[20] G. Zeydouni, M. Kianizadeh, Y. O. Khaniabadi et al., "Eriochrme black-T removal from aqueous environment by surfactant modified clay: equilibrium, kinetic, isotherm, and thermodynamic studies," *Toxin Reviews*, vol. 38, no. 4, pp. 307–317, 2019.

[21] E. N. El Qada, S. J. Allen, and G. M. Walker, "Adsorption of basic dyes onto activated carbon using microcolumns," *Industrial & Engineering Chemistry Research*, vol. 45, no. 17, pp. 6044–6049, 2006.

[22] M. A. Al-Ghouti and R. S. Al-Absi, "Mechanistic understanding of the adsorption and thermodynamic aspects of cationic methylene blue dye onto cellulosic olive stones biomass from wastewater," *Scientific Reports*, vol. 10, no. 1, article 15928, 2020.

[23] M. N. Zafar, M. Amjad, M. Tabassum, I. Ahmad, and M. Zubair, "$SrFe_2O_4$ nanoferrites and $SrFe_2O_4$/ground eggshell nanocomposites: fast and efficient adsorbents for dyes removal," *Journal of Cleaner Production*, vol. 199, pp. 983–994, 2018.

[24] S. Kumari, A. A. Khan, A. Chowdhury, A. K. Bhakta, Z. Mekhalif, and S. Hussain, "Efficient and highly selective adsorption of cationic dyes and removal of ciprofloxacin antibiotic by surface modified nickel sulfide nanomaterials: kinetics, isotherm and adsorption mechanism," *Colloids and Surface A: Physicochemical and Engineering Aspects*, vol. 586, article 124264, 2020.

[25] C. A. Almeida, N. A. Debacher, A. J. Downs, L. Cottet, and C. A. Mello, "Removal of methylene blue from colored effluents by adsorption on montmorillonite clay," *Journal of Colloid and Interface Science*, vol. 332, no. 1, pp. 46–53, 2009.

[26] V. Vadivelan and K. V. Kumar, "Equilibrium, kinetics, mechanism, and process design for the sorption of methylene blue onto rice husk," *Journal of Colloid and Interface Science*, vol. 286, no. 1, pp. 90–100, 2005.

[27] R. Sabarish and G. Unnikrishnan, "PVA/PDADMAC/ZSM-5 zeolite hybrid matrix membranes for dye adsorption: fabrication, characterization, adsorption, kinetics, and antimicrobial properties," *Journal of Environmental Chemical Engineering*, vol. 6, no. 4, pp. 3860–3873, 2018.

[28] K. Pimraksa, N. Setthaya, M. Thala, P. Chindaprasirt, and M. Murayama, "Geopolymer/zeolite composite materials with adsorptive and photocatalytic properties for dye removal," *PLoS One*, vol. 15, no. 10, article e0241603, 2020.

[29] K. Kombaiah, J. J. Vijaya, L. J. Kennedy, M. Bououdina, R. J. Ramalingam, and H. A. al-Lohedan, "Comparative investigation on the structural, morphological, optical, and magnetic properties of $CoFe_2O_4$ nanoparticles," *Ceramics International*, vol. 43, no. 10, pp. 7682–7689, 2017.

[30] S. M. Momina and S. Isamil, "Study of the adsorption/desorption of MB dye solution using bentonite adsorbent coating,"

Journal of Water Process Engineering, vol. 34, article 101155, 2020.

[31] O. S. Bayomie, H. Kandeel, T. Shoeib, H. Yang, N. Youseff, and M. H. El-Sayed, "Novel approach for effective removal of methylene blue dye from water using fava bean peel waste," *Scientific Reports*, vol. 10, no. 1, p. 7824, 2020.

[32] F. Marrakchi, M. J. Ahmed, W. A. Khanday, M. Asif, and B. H. Hameed, "Mesoporous-activated carbon prepared from chitosan flakes via single-step sodium hydroxide activation for the adsorption of methylene blue," *International Journal of Biological Macromolecules*, vol. 98, pp. 233–239, 2017.

[33] A. H. Jawad, A. S. Abdulhameed, and M. S. Mastuli, "Acid-factionalized biomass material for methylene blue dye removal: a comprehensive adsorption and mechanism study," *Journal of Taibah University for Science*, vol. 14, no. 1, pp. 305–313, 2020.

[34] M. M. Swamy, B. M. Nagabhushana, R. H. Krishna, N. Kottam, R. S. Raveendra, and P. A. Prashanth, "Fast adsorptive removal of methylene blue dye from aqueous solution onto a wild carrot flower activated carbon: isotherms and kinetics studies," *Desalination and Water Treatment*, vol. 71, pp. 399–405, 2017.

[35] A. H. Jawad, R. A. Rashid, M. A. M. Ishak, and K. Ismail, "Adsorptive removal of methylene blue by chemically treated cellulosic waste banana (Musa sapientum) peels," *Journal of Taibah University for Science*, vol. 12, no. 6, pp. 809–819, 2018.